Magnon Bose–Einstein condensate based qubit calculus

Preprint · November 2021

DOI: 10.48550/arXiv.2111.06798

5 authors, including:

Morteza Mohseni
RPTU - Rheinland-Pfälzische Technische Universität Kaiserslautern Landau
55 PUBLICATIONS **660** CITATIONS
SEE PROFILE

Victor S. L'vov
Weizmann Institute of Science
345 PUBLICATIONS **10,223** CITATIONS
SEE PROFILE

Alexander A. Serga
RPTU - Rheinland-Pfälzische Technische Universität Kaiserslautern Landau
217 PUBLICATIONS **14,382** CITATIONS
SEE PROFILE

Burkard Hillebrands
RPTU - Rheinland-Pfälzische Technische Universität Kaiserslautern Landau
643 PUBLICATIONS **32,777** CITATIONS
SEE PROFILE

Magnon Bose–Einstein condensate based qubit calculus

Morteza Mohseni, Vitaliy I. Vasyuchka, Victor S. L'vov, Alexander A. Serga, and Burkard Hillebrands
Fachbereich Physik and Landesforschungszentrum OPTIMAS, Technische Universität Kaiserslautern, Kaiserslautern 67663, Germany

Abstract

We propose to enable a set of room-temperature quantum computing functionalities using two room-temperature magnon Bose–Einstein condensates (BECs) existing at two distinct wavevectors in an Yttrium-Iron-Garnet ferrimagnetic film. The macroscopic wavefunctions of the two BECs, which have a group velocity of zero and are therefore stationary, serve as the two orthonormal basis states that form a qubit. Using the Gross-Pitaevskii equation and numerical simulations based on the Landau-Lifshitz-Gilbert equation, we first show how to initialize the qubit in one of the basis states: using wavevector-selective parallel parametric pumping enables the formation of only a single magnon BEC in one of the two lowest energy states of the system. Next, by translating the concept of Rabi-oscillations into the wavevector domain, we demonstrate how to manipulate the qubit state along the polar axis in the Bloch sphere representation. We also discuss the manipulation regarding the azimuthal angle.

Introduction

There is an enormous need for faster and more efficient information processing. Quantum computing is widely discussed as a future computing technology, especially with regard to computing power and the very favorable scaling properties [1-8]. However, current quantum computing technologies are still far from ubiquitous. In particular, the need to operate in the milli-Kelvin temperature range is a significant obstacle.

In the field of quantum information science, the basic unit of information is defined as a quantum bit or qubit for short [3-4, 9-11]. The qubit is most often represented by a superposition of two wavefunctions, which describe the two orthonormal basis states of the system. Thus, due to the interference of these two wavefunctions, a qubits is multivalued with the independent continuous parameters of the wavefunction's amplitudes and the relative phase. Qubits are regularly represented as states on the surface of a Bloch sphere, see Fig. 1(a).

In the search for physical systems suitable to represent a set of qubits, macroscopic quantum states of matter such as Bose-Einstein condensates (BEC) are excellent candidates, in particular due to their inherent coherency [7, 12-17]. The BEC is a collective quantum state, in which particles represented by a coherent wavefunction – in this case magnons – populate a lowest energy state of the system [18- 23]. Such a BEC can be created using magnons in ferrimagnetic crystals [24-38].

The work presented here addresses room-temperature, magnon-BEC based qubit calculus. At room temperature, magnon BECs operate in the semiclassical regime, and some effects that exist only in the quantum mechanical regime, such as entanglement of states, are not accessible. However, a rather large subset of architectural aspects, algorithms, and *modi operandi* used in quantum-mechanical computing can be adapted and

made operational. Many algorithms do not rely on quantum mechanical entanglement [39, 40] and can be implemented with the semiclassical qubit functionality discussed here. This approach removes the technical obstacles that exist in quantum mechanical calculations, such as the need to operate at milli-Kelvin temperatures, and allows operation in a room-temperature solid-state device with standard microwave interface technology.

An important issue in this context is scaling. Quantum computing claims polynomial scaling of computation time with system size, which is very advantageous over the merely exponential scaling properties of conventional, classical Boolean logic. Recently, it has been shown that polynomial scaling holds for a number of algorithms that use wave-based computing in a non-quantum mechanical implementation (see e.g. Ref. [41, 42]). Thus, in terms of computation time, there is a fairly favorable gap between classical Boolean and true quantum-mechanical computing concepts, which can be filled by the magnon qubit concept presented here.

Magnon BECs and magnon BEC qubits

The magnon BEC phenomenon addresses the spontaneous formation of a coherent state or wave — a macroscopic quantum state — in an otherwise disordered magnonic system. At room temperature, a magnon BEC can form in a weakly interacting magnon gas if the chemical potential of the system is increased to the minimum magnon energy, for example by increasing the magnon density via external injection [25-28]. The most prominent method to inject magnons is parallel parametric pumping [29,30], in which external microwave photons of frequency ω_p and wavenumber $q_\mathrm{p} \simeq 0$ split into two magnons with the frequency $\omega_\mathrm{m} = \omega_\mathrm{p}/2$ and wavevectors $\pm\boldsymbol{q}_\mathrm{m}$. The overpopulated magnon gas near the bottom of the magnon spectrum relaxes to the two lowest energy states via multi-magnon scattering processes, forming magnon BECs in the two global minima of the system as shown in Fig. 1(b). The observed exciting dynamics of such magnon BECs, such as their inherent coherency, quantized vorticity, supercurrents, Bogoliubov waves, and Josephson oscillations, all at room temperature [30-38], are further encouraging to consider magnon BECs for performing qubit computing operations.

We take into account the fact that for a film, in the two-dimensional in-plane wavevector landscape, the magnon frequency spectrum $\omega = \omega(q)$ has two minima at symmetric values of the wavevectors, $\pm\boldsymbol{q}_\mathrm{BEC}$, see Fig. 1(b). Consequently, the condensate consists of two components, BEC^+ and BEC^-,described by the wavefunctions $\Psi^+(x,t)\exp\left[i\left(q_{\mathrm{BEC}}x - \omega_{\mathrm{BEC}}t\right)\right]$ and $\Psi^-(x,t)\ \exp\left[i\left(-q_{\mathrm{BEC}}x - \omega_{\mathrm{BEC}}t\right)\right]$, respectively. The fundamental basis for the description of the phenomena in this semi-classical limit is the nonlinear Schrödinger equation (NSE), also known as the Gross-Pitaevskii equation (GPE) [43]. In the one-dimensional version, which is fully applicable here, it reads

$$\left[i\frac{\partial}{\partial t} + D_{xx}\frac{\partial^2}{\partial x^2} \quad -T|\Psi^+|^2 - S|\Psi^-|^2 - P^+(x,t) + i\Gamma\right]\cdot\Psi^+(x,t) = iF^+(x,t), \tag{1a}$$

$$\left[i\frac{\partial}{\partial t} + D_{xx}\frac{\partial^2}{\partial x^2} \quad -T|\Psi^-|^2 - S|\Psi^+|^2 - P^-(x,t) + i\Gamma\right]\cdot\Psi^-(x,t) = iF^-(x,t). \tag{1b}$$

Here, $D_{xx} = \frac{1}{2}\frac{\partial^2\omega(\boldsymbol{q})}{\partial q_x^2}$ is the dispersion coefficient in the x-direction, and T and S are the amplitudes of self- and cross-interactions between BEC^+ and BEC^-, respectively. $P^{\pm}(x,t)$ are the external potentials caused, for instance, by variations of longitudinal magnetizing fields, and $F^{\pm}(x,t)$ are the external forces caused, e.g., by transversal microwave magnetic fields. The magnon relaxation rate, originating, for example, from the interaction with the phonon bath, is denoted by Γ. For $\Gamma = 0$, Eq. (1) has stationary solutions, which describe the two magnon BECs at the bottom of the spin-wave spectrum in the $+q_{\mathrm{BEC}}$ and $-q_{\mathrm{BEC}}$ positions. If $\Gamma \neq 0$, the wavefunctions $\Psi^{\pm}(x,t)$ decay as $\exp(-\Gamma t)$.

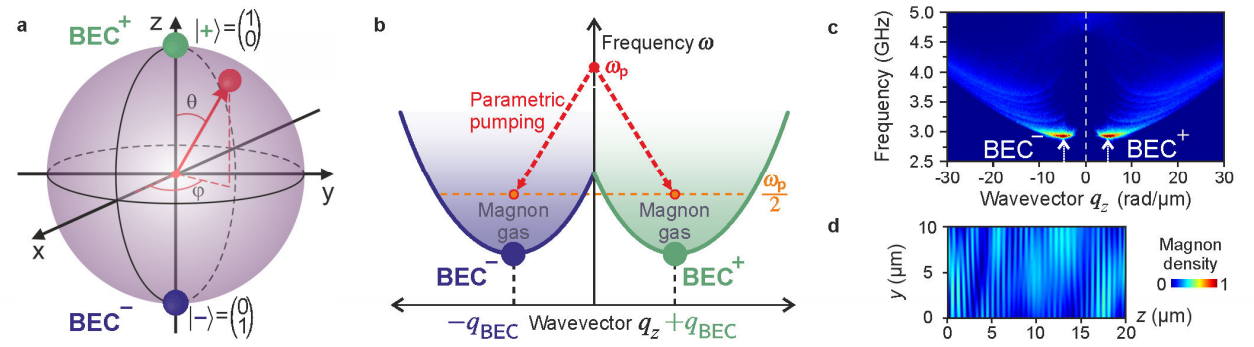

FIG. 1. a) A magnon BEC qubit (red dot) on the surface of a Bloch sphere. The $|+\rangle$ and $|-\rangle$ states representing BEC^+ and BEC^- are indicated by the green and blue dots at the north and south pole. b) Schematic spectrum of the magnon dispersion and BEC generation via parametric pumping using $q \approx 0$ microwave photons. c) Numerical simulation of the condensation process of parametrically populated magnon gas in a YIG ferrimagnetic film. The fine structure of the magnon gas population corresponds to the thickness magnon modes of this film. The YIG film-thickness is 5 μm. The pumping frequency is 7.5 GHz with a pump duration of 50 ns. The bias magnetic field is 100 mT. d) Spatial interference pattern formed by BEC^+ and BEC^-.

In the space-homogeneous case, there is, apart from the oscillating factor $\exp\left[i\left(q_{\mathrm{BEC}}x\right)\right]$, no x-dependence, and Eq. (1) becomes identical to the general form of a degenerate two-level system. An example of such a system is a quantum particle (qp) with spin $S = ½$, which has a wavefunction consisting of a spin-up (ψ_{qp}^{+}) and a spin-down (ψ_{qp}^{-}) component. To stress this analogy, we introduce the normalized BEC wavefunctions

$$\psi^{\pm}(x,t) = \Psi^{\pm}(x,t)/\sqrt{|\Psi^{+}(x,t)|^2 + |\Psi^{-}(x,t)|^2}\,, \tag{2a}$$

$$|\psi^{+}(x,t)|^2 + |\psi^{-}(x,t)|^2 = 1\,. \tag{2b}$$

We propose the system consisting of the two magnon BECs as a semi-classical analogue of the quantum bit (qubit) used in quantum computing. The qubit state position on the Bloch sphere (see Fig. 1a) is given by the polar angle θ and azimuthal angle φ. They are defined by the normalized densities of the two BECs,

$N^{\pm} = |\psi^{\pm}(x,t)|^2$ with

$$N^{+}(x,t) + N^{-}(x,t) = 1\,, \tag{3a}$$

$$\theta = \mathrm{Arccos}[(N^{+}(x,t) - N^{-}(x,t))/2], \tag{3b}$$

$$\varphi = \mathrm{Arg}[\psi^{+}(x,t) \cdot \psi^{-*}(x,t)]. \tag{3c}$$

Thus, any qubit state on the Bloch sphere can be addressed. To this end, we need to demonstrate the capability to control i) the number of magnons in each of the two BECs, and ii) their relative phase, which will be discussed in the following and demonstrated using numerical simulations [44-45].

Results

Initialization of magnonic qubit states at the equator of the Bloch sphere

A convenient way to generate a magnon BEC is to use the parametric excitation mechanism by a space-homogeneous electromagnetic field for generation of magnons in the gaseous magnon regime and to let these magnons condense into the BEC states via dominating four-magnon-scattering events [25-26]. Due to the momentum conservation during the magnon thermalization processes, the resulting numbers of BEC^{+} and BEC^{-} also remain the same, $N^{+} = N^{-}$, as it is evidenced by numerous magnon BEC experiments [25-27] and by results of numerical modeling shown in Fig. 1d. It means that such a prepared initial magnon qubit state lies somewhere on the equator of the Bloch sphere, $\cos\theta = 0$, and the azimuthal angle ϕ has an arbitrary value (further below we will address how to control ϕ). We note that the coherency of the generated BECs is evidenced by the spatial interference pattern of the two condensates, as observed experimentally [31], and shown by our micromagnetic simulations displayed in Fig. 1d. Despite the presence of small nonuniformities in the spatial interference pattern evidencing the existence of quantized vorticities, the coherency of the two BECs on the larger scale is preserved [31, 36, 38, 46].

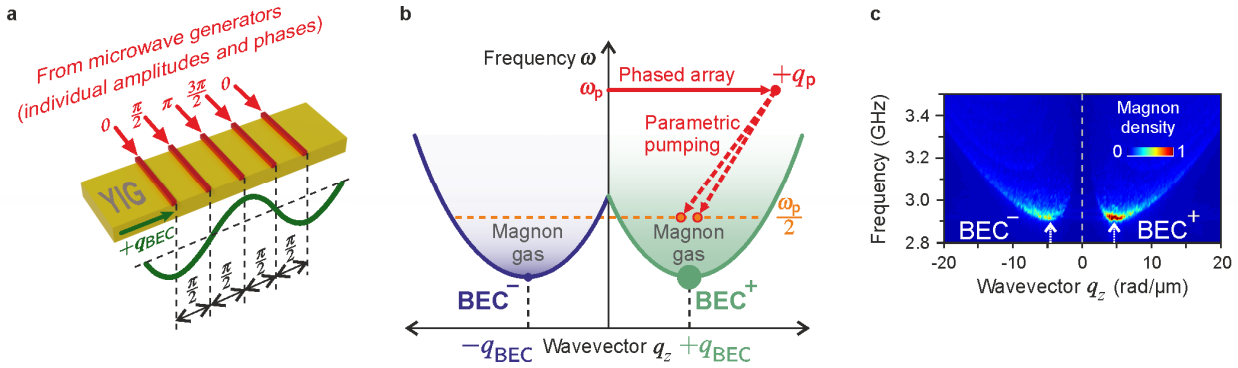

FIG. 2. Wavevector-selective parametric pumping scheme and formation of an asymmetric magnon BEC. a) Phased-array magnetic field excitation mechanism. b) Schematic view of wavevector-selective parametric pumping scheme. c) Micromagnetic modeling of BEC formation in a parametrically populated magnon gas. The color code indicates the normalized magnon density.

Initialization of magnon qubits states at the poles and any latitude of the Bloch sphere.

We propose to use a moving periodic pattern of a microwave magnetic field in order to pump magnon pairs dominantly to the positive or negative half of the wavevector space. It acts like an artificial propagating microwave field with controlled wavevector and frequency. This moving pattern can be created by an array of L parallel wires separated by a distance a and connected to a set of phase-locked microwave generators operating at the pumping frequency ω_p, see Fig. 2a. They work analogous to a phased array [47, 48]: The phases of the signals applied to the wires are chosen such that the phase difference Δ_wire between neighbored wires is fixed to $\Delta_\mathrm{wire} = 2\pi/K$ with K being an integer number. Thus, moving magnetic field patterns are generated, which oscillate with ω_p and propagate with wavevector $|\boldsymbol{q}_\mathrm{p}| = 2\pi/Ka$. For $K > 2$ the field pattern has a well-defined unique direction of propagation, which is indicated by the sign of Δ_wire.

Such a field pattern, which can be characterized by a reciprocal lattice vector $|\boldsymbol{q}_\mathrm{p}| = 2\pi/Ka$ pointing into the direction of motion and the microwave frequency ω_p, will pump two co-propagating magnons with frequencies $\omega_\mathrm{p}/2$ and wavevectors $q_\mathrm{p} = 2q_\mathrm{m}$, $\boldsymbol{q}_\mathrm{m} \parallel \boldsymbol{q}_\mathrm{p}$. In this scenario, the thermalization of the parametric magnons will result in the population of either BEC^- or BEC^+. This means that the prepared initial state of the magnon qubit is either at the north or south pole of the Bloch sphere. By proper choice of $\boldsymbol{q}_\mathrm{p}$, it is possible to populate BEC^+ and BEC^- with predefined densities N^+ and N^-, i.e., to adjust the polar angle of the magnon qubit. The validity of this approach is demonstrated by the results of our micromagnetic simulations as shown in Fig. 2c.

Single-qubit protocols using Rabi-like oscillations

Achieving a controlled change in the state of the previously initialized magnon qubit, e.g., transformation of BEC^+ into BEC^- and vice versa, and addressing any intermediate state, is essential for computing. Indeed, our objective is to realize unitary transformations of the qubit in the two-dimensional Hilbert space to resemble logic state operations. The following tools and approaches serve as key ingredients for implementing the functionalities of the Pauli-X and -Z gates and the Hadamard gate. For this purpose, we use the concept of Rabi-oscillations, which refers to a cyclic energy exchange in a two-level quantum system in the presence of a driving field [49-51]. The magnon qubit represents the analogy of a two-level system in the wavevector domain, and thus, we translate the Rabi cycle into this domain as discussed in the following.

Let us consider the magnon qubit initialized in the north pole state, i.e., at BEC^+, as shown in Fig. 2c. Instead of a time-dependent field, here we use a space-dependent stationary magnetic field to induce a Rabi cycle between the two BEC wavevector components. This field is generated using a dynamic magnonic crystal (MC) [51] similar to the setup that is shown in Fig. 2a. However, instead of a phased array driven by microwave currents, we insert DC currents into the wires to control the bias magnetic field. Consequently, this changes the energy landscape of the system. Once this MC is turned on, it creates a gap in the magnon dispersion relation at the wavevector corresponding to the periodicity of the crystal. This leads to a Bragg reflection of the incoming

magnons at that particular wavevector, which in our case is q_{BEC} [53]. However, if the magnons already exist in the system and the MC is switched on, geometrically-induced coupling between the existing magnons and the MC leads to the oscillations of the magnons between the opposite wavevector-states given their equivalent frequencies [53].

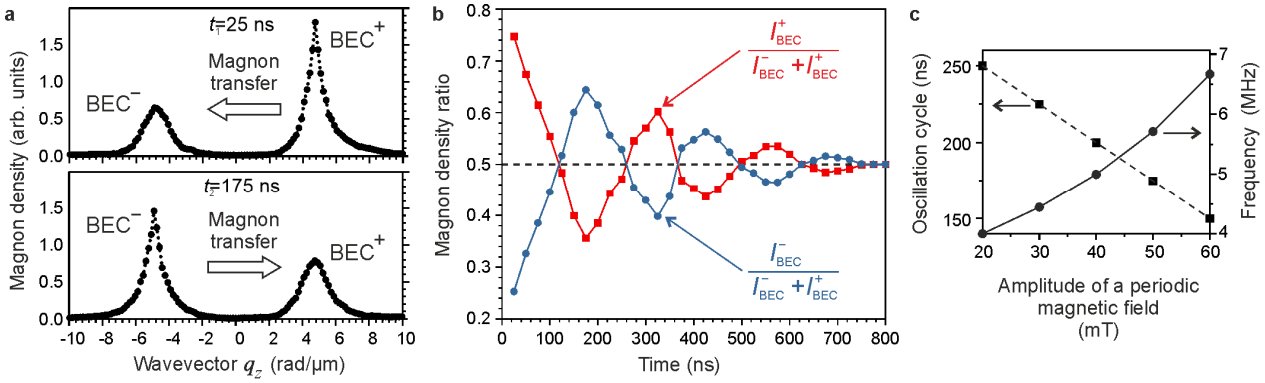

FIG. 3. Rabi oscillations in magnon BEC within a magnonic crystal. a) Wavenumber-dependent distribution of the magnon density at the bottom of spin-wave spectrum for two moments of time. b) Peak magnon densities at $+q_{\mathrm{BEC}}$ and $-q_{\mathrm{BEC}}$ as functions of time. c) Periodicity of the Rabi oscillations as a function of the amplitude of a spatially-periodic magnetic field induced by the dynamic magnonic crystal.

In a numerical simulation experiment, we activate the MC once the magnon qubit at BEC^+ is established. Figure 3a shows the distribution of the condensed magnon density at the wavevector space in two given time spans. During the course of time from, e.g., t_1 = 25 ns to t_2 = 175 ns, the magnons are transferred from BEC^+ to BEC^-. The oscillation cycle is more visible in Fig. 3b, which represents the normalized magnon densities at BEC^- and BEC^+ as a function of time. Interestingly, the oscillations between the two condensates continue until the condensed magnons dissipate due to the magnetic damping. Moreover, the oscillation cycle can be tuned using the MC modulation amplitude, i.e., by the amplitude of the spatially periodic magnetic field produced by the MC. As shown in Fig. 3c, increasing the MC amplitude leads to shorter oscillation cycles, and consequently higher oscillations frequencies. This can be understood by a stronger coupling of the magnons and the MC [53]. Indeed, the repetition of this action turns the magnon qubit back into its initial state, thus representing the bit-flip operation described by the Pauli X matrix, $X = \begin{bmatrix} 0 & 1 \\ 1 & 0 \end{bmatrix}$. By changing the oscillation cycles, it is also possible to transfer the system to a superposition of BEC^+ and BEC^-, characterized by finite densities of both BECs. The proposed and demonstrated mechanism not only further suggests the coherency of the generated condensates, but also provides a strong tool to manipulate the magnon qubit states on the Bloch sphere even as a function of time, which is an additional degree of freedom for this purpose.

Furthermore, controlling the azimuthal angle of the qubit is essential as well. This is possible by controlling

the relative phase between the two BECs. By inserting a low-frequency microwave RF field with a linewidth smaller than the linewidth of the BEC into a structure similar to the one used to realize the dynamic MC, it is possible to change the phase of the BEC and consequently the position of the qubit on the Bloch sphere. We emphasize that patterning such structures is a task that can be accomplished with today's nanostructuring techniques.

The dynamic MC can be optimized for simultaneous work with phase-adjusted RF and pulsed DC-signals. This allows one to manipulate both the polar and azimuthal angles of a qubit state, and, by extension, to pave the way towards implementation of various phase-shift gates. For example, as an outlook, we expect the implementation of the Pauli-Z gate, represented by the Pauli-Z matrix, $Z = \begin{bmatrix} 1 & 0 \\ 0 & -1 \end{bmatrix}$. By having the possibility of controlled rotation in relation to the different axes of the Bloch's sphere, the functionality of the Hadamard gate, $H = \frac{1}{\sqrt{2}} \begin{bmatrix} 1 & 1 \\ 1 & -1 \end{bmatrix}$ can be achieved.

Conclusions and outlook

The aim of the presented study is to demonstrate, that qubit calculus is feasible using magnon BECs at room temperature. Our work might initiate a new direction in the field of magnonics by bridging the field of macroscopic quantum states of magnons and quantum computing functionalities [54-56]. We have used two spatially overlapping and interfering stationary magnon BECs with opposite wavevectors for qubit implementation. We presented the wavevector-selective parallel pumping mechanism for qubit initialization at the north or south pole of the Bloch sphere. Moreover, we have shown that Rabi-like oscillations can be translated into the wavevector domain to manipulate the magnon qubit states on the Bloch sphere. Realistic numerical simulations close to the experimental conditions provide evidence for the feasibility of this approach and they also shed light on the proposed mechanisms.

As an outlook, the next steps to be taken are obvious: It is the realization of coupling of two and more magnon qubits. Coupling of spatially separate magnon BECs has been already demonstrated leading to the phenomenon of magnon Josephson oscillations [34, 57]. Next, this must be translated into the coupling of magnon qubits. Microwave antenna structures for the phase coherent detection and generation of magnon BECs can be used to coherently couple two or more magnon qubits over larger spatial distances. In summary, there are good prospects for realizing qubit-based computations with Magnon BECs.

Methods

Solving the equation of the magnetization motion have been carried out numerically using the open source MuMax 3.0 package. It uses the Dormand-Prince method [44] for the integration of the Landau-Lifshitz-Gilbert (LLG) equation:

$$\frac{d\mathbf{M}}{dt} = -|\gamma|\mathbf{M}\times\mathbf{B}_{\text{eff}} + \frac{\alpha}{M_s}\left(\mathbf{M}\times\frac{d\mathbf{M}}{dt}\right) \quad (4)$$

in which **M** is the magnetization vector, $\mathbf{B}_{\text{eff}}$ is the effective magnetic field, γ is the gyromagnetic ratio, and α is the damping constant. The system under investigation is a film with dimensions of 51.2 µm × 25.6 µm × 5 µm that is divided into 1024× 512 ×16 cells. An external magnetic film is applied in the plane with an amplitude of 100 mT. Realistic magnetic parameters of the YIG film are used: M_s = 140 kA/m, α = 0.0002, A_{exch} = 3.5 pJ/m [25, 45-46]. Magnons are injected using parallel parametric pumping, in which microwave photons of frequency of ω_p = 7.5 GHz generate magnons with the frequency $\omega_p/2$ = 3.75 GHz. The duration of the pumping pulse is fixed to t_{pumping} = 50 ns in all simulations, and the system is then relaxed toward its equilibrium state to permit the BEC to establish at the bottom of the magnon spectrum. All simulations have been carried assuming room temperature. The used setup in this study resembles typical conditions of real experiments [25, 26].

In principle, we have carried out the micromagnetic simulations based on two steps. First, the external field is applied in the film plane to establish the relaxed magnetization state. This state is consequently used as the ground state in the dynamic simulations, in which parallel parametric pumped magnons are generated using an oscillating field which is applied parallel to the static field. The dynamic components of the magnetization, $M(x,y,z,t)$ of each cell are collected over a period of time. In order to process the raw data, one and two-dimensional fast Fourier transformation (FFT) has been carried out on the collected data set [45].

References and notes

1 F. Arute et al., Quantum supremacy using a programmable superconducting processor, *Nature* **574**, 505 (2019).

2 P. Kok, W. J. Munro, K. Nemoto, T. C. Ralph, J. P. Dowling, G. J. Milburn, Linear optical quantum computing with photonic qubits, *Rev. Mod. Phys*. **79**, 135 (2007).

3 D. A. Meyer, Quantum computing classical physics, *Philos. Trans. R. Soc. A*. **360**, 395 (2002).

4 M. A. Nielsen I. L. Chuang, *Quantum Computation and Quantum Information* (Cambridge University Press, 2010).

5 C. P. Williams, *Explorations in Quantum Computing* (Springer, London, 2011).

6 T. D. Ladd, F. Jelezko, R. Laflamme, Y. Nakamura, C. Monroe, J. L. O'Brien, Quantum computers, *Nature* **464**, 45 (2010).

7 Y. Makhlin, G. Schan, A. Shnirman, Quantum-state engineering with Josephson-junction devices, *Rev. Mod. Phys*. **73**, 357 (2001).

8 J. L. O'Brien, Optical quantum computing, *Science* **318**, 1567 (2008).

9 I. H. Deutsch, Harnessing the power of the second quantum revolution, *PRX Quantum*. **1**, 020101 (2020).

10 J.D. Hidary, *Quantum Computing: An Applied Approach* (Springer International Publishing, 2019)

11 C.-R. Wie, Two-qubit Bloch sphere, *Physics*. **1**, 020101 (2020).

12 A. Qaiumzadeh, H. Skarsvåg, C. Holmqvist, A. Brataas, Spin superfluidity in biaxial antiferromagnetic insulators, *Phys. Rev. Lett*. **118**, 137201 (2017)

13 Y. Tserkovnyak M. Kläui, Exploiting coherence in nonlinear spin-superfluid transport, *Phys. Rev. Lett*. **119**, 187705 (2017).

14 T. Byrnes Y. Yamamoto, Macroscopic quantum computation using Bose–Einstein condensates, *Phys. Rev. A* **85**, 040306(R) (2012).

15 S. N. Adrianov S. A. Moiseev, Magnon qubit and quantum computing on magnon Bose–Einstein condensates, *Phys. Rev. A* **90**, 042303 (2014).

16 N. Mohseni, M. Narozniak, A. N. Pyrkov, V. Ivannikov, J. P. Dowling & T. Byrnes, Error suppression in adiabatic quantum computing with qubit ensembles, *npj Quantum Information* **7**, 71 (2021)

17 H. Semenenko, T. Byrnes, Implementing the Deutsch-Jozsa algorithm with macroscopic ensembles, *Phys. Rev. A* **93**, 052302 (2016)

18 A. D. Stone, *Einstein and the quantum: The quest of the valiant Swabian* (Princeton University Press, 2015).

19 A. Einstein, Quantentheorie des einatomigen idealen Gases, Sitzungsber. *Preuss. Akad. Wiss. Phys.-math. Kl*. **22**, 261 (1924).

20 K. B. Davis, M.-O. Mewes, M. R. Andrews, N. J. van Druten, D. S. Durfee, D. M. Kurn, W. Ketterle, Bose-Einstein condensation in a gas of sodium atoms, *Phys. Rev. Lett*. **75**, 3969–3973 (1995).

21 A. Amo, J. Lefrère, S. Pigeon, C. Adrados, C. Ciuti, I. Carusotto, R. Houdré, E. Giacobino, A. Bramati, Superfluidity of polaritons in semiconductor microcavities, *Nat. Phys*. **5**, 805–810 (2009).

22 J. P. Eisenstein A. H. MacDonald, Bose-Einstein condensation of excitons in bilayer electron systems, *Nature* **432**, 691–694 (2004).

23 J. Klaers, J. Schmitt, F. Vewinger, M. Weitz, Bose–Einstein condensation of photons in an optical microcavity, *Nature* **468**, 545–548 (2010).

24 Yu. M. Bunkov G. E. Volovik, Bose–Einstein condensation of magnons in superfluid ^{3}He. *J. Low Temp. Phys*. **150**, 135–144 (2008).

25 S. O. Demokritov, V. E. Demidov, O. Dzyapko, G. A. Melkov, A. A. Serga, B. Hillebrands, A. N. Slavin, Bose-Einstein condensation of quasi-equilibrium magnons at room temperature under pumping, *Nature* **443**, 430–433 (2006).

26 A. A. Serga, V. S. Tiberkevich, C. W. Sandweg, V. I. Vasyuchka, D. A. Bozhko, A. V. Chumak, T. Neumann, B. Obry, G. A. Melkov, A. N. Slavin, B. Hillebrands, Bose–Einstein condensation in an ultra-hot gas of pumped magnons, *Nat. Commun*. **5**, 3452 (2014).

27 M. Schneider, T. Brächer, D. Breitbach, V. Lauer, P. Pirro, D. A. Bozhko, H. Yu. Musiienko-Shmarova, B. Heinz, Q. Wang, T. Meyer, F. Heussner, S. Keller, E. Th. Papaioannou, B. Lägel, T. Löber, C. Dubs, A. N. Slavin, V. S. Tiberkevich, A. A. Serga, B. Hillebrands, A. V. Chumak, Bose-Einstein condensation of quasiparticles by rapid cooling, *Nat. Nanotech*. **15**, 457 (2020).

28 C. Safranski, I. Barsukov, H. K. Lee, T. Schneider, A. A. Jara, A. Smith, H. Chang, K. Lenz, J. Lindner, Y. Tserkovnyak, M. Wu, I. N. Krivorotov, *Nat. Comm.* ***8***, 117 (2017)

29 E. Schlömann, Longitudinal susceptibility of ferromagnets in strong rf fields, *J. Appl. Phys*. **33**, 527 (1962).

30 V. S. L'vov, *Wave Turbulence Under Parametric Excitation: Applications to Magnets* (Springer, Berlin, 1994).

31 P. Nowik-Boltyk, O. Dzyapko, V. E. Demidov, N. G. Berloff, S. O. Demokritov, Spatially non-uniform ground

stte and quantized vortices in a two-component Bose-Einstein condensate of magnons, *Sci. Rep.* **2**, 482 (2012).

32 D. A. Bozhko, A. A. Serga, P. Clausen, V. I. Vasyuchka, F. Heussner, G. A. Melkov, A. Pomyalov, V. S. L'vov, B. Hillebrands, Supercurrent in a room-temperature Bose-Einstein magnon condensate, *Nat. Phys.* **12**, 1027 (2016).

33 D. A. Bozhko, A. J. E. Kreil, H. Yu. Musiienko-Shmarova, A. A. Serga, A. Pomyalov, V. S. L'vov, B. Hillebrands, Bogoliubov waves and distant transport of magnon condensate at room temperature, *Nat. Commun*. **10**, 2460 (2019).

34 A. J. E. Kreil, A. Pomyalov, V. S. L'vov, H. Yu. Musiienko-Shmarova, G. A. Melkov, A. A. Serga, B. Hillebrands, Josephson oscillations in a room-temperature Bose–Einstein magnon condensate, arXiv:1911.07802 (2020).

35 K. Nakata, K. A. van Hoogdalem, P. Simon, D. Loss, Josephson and persistent spin currents in Bose-Einstein condensates of magnons, *Phys. Rev. B* **90**, 144419 (2014)

36 V. E. Demidov, O. Dzyapko, S. O. Demokritov, G. A. Melkov, A. N. Slavin, Observation of spontaneous coherence in Bose-Einstein condensate of magnons, *Phys.Rev. Lett*. **100**, 047205 (2008).

37 A. I. Bugrij V. M. Loktev, On the Theory of Spatially Inhomogeneous Bose-Einstein Condensation of Magnons in Yttrium Iron Garnet, *Low Temp. Phys*. **39**, 1037 (2013).

38 T. B. Noack, V. I. Vasyuchka, A. Pomyalov, V. S. L'vov, A. A. Serga, B. Hillebrands, Evolution of room-temperature magnon gas: Toward a coherent Bose-Einstein condensate, *Phys. Rev. B* **104**, L100410 (2021).

39 E. Biham, G. Brassard, D. Kenigsberg, T. Mor, Quantum computing without entanglement, *Theor. Comput. Sci.* **320**, 15 (2004).

40 B. P. Lanyon, M. Barbieri, M.P. Almeida, A.G. White, Experimental quantum computing without entanglement, *Phys. Rev. Lett*. **101**, 200501 (2008).

41 M. Balynsky, H. Chiang, D. Gutierrez, A. Kozhevnikov, Y. Filimonov, and A. Khitun, Quantum computing without quantum computers: Database search and dataprocessing using classical wave superposition, *J. Appl. Phys.* **130**, 164903 (2021)

42 K. Cheng, Y. Fan, W. Zhang, Y. Gong, S. Fei, and H. Li, Optical Realization of Wave-Based Analog Computing with Metamaterials, *Appl. Sci.* **11**, 141 (2020).

43 L. P. Pitaevskii, Bose–Einstein condensation in magnetic traps. Introduction to the theory, *Phys. Usp*. **41**, 569 (1998).

44 A. Vansteenkiste, J. Leliaert, M. Dvornik, M. Helsen, F. Garcia-Sanchez, B. Van Waeyenberge, The design and verification of MuMax3, *AIP Advances* **4**, 107133 (2014).

45 M. Mohseni, A. Qaiumzadeh, A. A. Serga, A. Brataas, B. Hillebrands, P. Pirro, Bose–Einstein condensation of nonequilibrium magnons in confined systems, *New J. Phys*. **22**, 083080 (2020).

46 S. M. Rezende, Theory of coherence in Bose–Einstein condensation phenomena in a microwave-driven interacting magnon gas, *Phys. Rev. B* **79**, 174411 (2009).

47 H. J. Visser, *Array and Phased Array Antenna Basics* (John Wiley Sons, 2006).

48 H. J. Visser, *Modern Antenna Design, 2nd Ed.* (John Wiley Sons, 2005).

49 D. Griffiths, *Introduction to Quantum Mechanics, 2nd Ed.* (Pearson Prentice Hall, 2005).

50 Y. O. Dudin, L. Li, F. Bariani, A. Kuzmich, Observation of coherent many-body Rabi oscillations, *Nat. Phys*. **8**,

790-794 (2012).

51 N. N. Rosanov, Nonlinear Rabi oscillations in a Bose–Einstein condensate, *Phys. Rev. A.* **88**, 063616 (2013).

52 A.V. Chumak, V. S. Tiberkevich, A. D. Karenowska, A. A. Serga, J. F. Gregg, A. N. Slavin, B. Hillebrands, All-linear time reversal by a dynamic artificial crystal, *Nat. Comm*. **1**, 141 (2010)

53 A. D. Karenowska, V. S. Tiberkevich, A. V. Chumak, A. A. Serga, J. F. Gregg, A. N. Slavin, B. Hillebrands, Oscillatory energy exchange between waves coupled by a dynamic artificial crystal, *Phys. Rev. Lett*. **108**, 015505 (2012).

54 M. Elyasi, Y. M. Blanter, G. E. W. Bauer, Resources of nonlinear cavity magnonics for quantum information, *Phys. Rev. B* **101**, 054402 (2020).

55 Y. Tabuchi, S. Ishino, A. Noguchi, T. Ishikawa, R. Yamazaki, K. Usami, Y. Nakamura, Coherent coupling between a ferromagnetic magnon and a superconducting qubit, *Science* **349**, 405 (2015).

56 D. Lachance-Quirion, S. P. Wolski, Y. Tabuchi, S. Kono, K. Usami, Y. Nakamura, Entanglement-based single-shot detection of a single magnon with a superconducting qubit, *Science* **367**, 425 (2020).

57 K. G. Fripp, V. V. Kruglyak, Spin-wave wells revisited: From wavelength conversion and Möbius modes to magnon valleytronics, *Phys. Rev. B* **103**, 184403 (2021)

Acknowledgements

Funding: This research was funded by the European Research Council within the Advanced Grant No. 694709 SuperMagnonics and by the Deutsche Forschungsgemeinschaft (DFG, German Research Foundation) within the Transregional Collaborative Research Center – TRR 173 – 268565370 “Spin+X” (projects B01, B04).

Author Contributions: M. M. performed the numerical simulations, analyzed the data. V. V., V. L. and A. S. devised and planned the project and analyzed the general analytical model. B. H. led the project. All authors discussed the results and contributed to writing the manuscript.

Author Information

Correspondence and requests for materials should be addressed to Burkard Hillebrands. (hilleb@physik.uni-kl.de).